


UDC 550.42

Composition Heterogeneity of Xenoliths of Mantle Peridotites from Alkaline Basalts of the Sverre Volcano, the Svalbard Archipelago

Dmitriy S. ASHIKHMIN¹, Sergey G. SKUBLOV² 

¹ *A.P.Karpinsky Russian Geological Research Institute, Saint-Petersburg, Russia*

² *Institute of Precambrian Geology and Geochronology RAS, Saint-Petersburg, Russia*

The article presents the results of a study of the composition of xenoliths of mantle peridotites (seven samples), collected from the Quaternary basalts of the Sverre volcano, the Svalbard archipelago. The presence of two big (more than 15 cm in diameter) xenoliths of spinel lherzolite allowed us to consider a change in their composition in the central, intermediate, and marginal parts of the samples.

It is proposed to distinguish three types of xenoliths by the distribution of trace and rare earth elements. Enrichment of mantle peridotites with light rare earth elements, as well as high field strength (HFS) and large-ion lithophile (LIL) elements, is presumably associated with mantle metasomatism.

Key words: mantle xenoliths; mantle metasomatism; peridotite; trace elements; rare earth elements; Svalbard

Acknowledgments. The study was performed with the financial support of the Russian Foundation for Basic Research (grant 19-35-50014) within the IPGG RAS research scientific work № 0153-2019-0002. The authors are grateful to O.L. Galankina (IPGG RAS), S.G. Simakin, and E.V. Potapov (Valiev Institute of Physics and Technology of RAS, Yaroslavl branch) for carrying out the analytical work.

How to cite this article: Ashikhmin D.S., Skublov S.G. Composition Heterogeneity of Xenoliths of Mantle Peridotites from Alkaline Basalts of the Sverre Volcano, the Svalbard Archipelago. *Journal of Mining Institute*. 2019. Vol. 239, p. 483-491. DOI: 10.31897/PMI.2019.5.483

Introduction. Currently, due to the systematic study of mantle xenoliths, significant information on the Earth deep structure has been accumulated. Understanding the distribution of trace elements in xenoliths and rock-forming minerals can promote understanding the evolution of matter in the upper mantle, as well as shed light on the interaction of mantle rocks with deep alkaline melts [1, et al.]. In particular, data on the xenoliths composition are used to substantiate the hypotheses of the basalt genesis [5]. Mantle xenoliths found in various alkaline basaltoid provinces vary in the content of rare earth elements (REE). This is especially evident in the case of light rare earth elements. The heterogeneity in REE composition is observed not only when comparing samples from different provinces, but often within one province and even one xenoliths bearing object [3, 12].

Xenoliths of mantle peridotites delivered to the surface by alkaline basalts of the volcanic complex of the Svalbard archipelago have been studied in detail for a long time in the framework of mantle metasomatism and the evolution of mantle rocks [1, 2, 10, etc.]. Our study of the melt pockets in the central part of spinel peridotite xenolith have shown a change in the composition of olivine and clinopyroxene during the metasomatism of the carbonate melt with the formation of secondary minerals and silicate glass [1]. However, until recently, there has been no comparative study on the trace elements content in xenoliths from one field, and even less from different zones of large-sized samples, which according to published data are extremely rare in Svalbard. The reason for the enrichment of the xenoliths under study with incompatible elements remains debatable: either this is a consequence of mantle metasomatism or the effect of transporting basaltic melts.

The paper presents the results of a study of the composition of xenoliths of mantle peridotites (7 samples), collected from the Quaternary basalts of the Sverre volcano, the Svalbard archipelago. The presence of two big (more than 15 cm in diameter) xenoliths of spinel lherzolites allowed a comparative analysis of the composition in the central, intermediate, and marginal parts of the samples.

In our previous studies we have shown that xenoliths, before being extracted to the surface by quaternary alkaline basaltic melts, underwent a series of transformations while the rocks were in the mantle [1, 2]. Spinel lherzolites were impacted by at least two significant processes: depletion caused by partial melting, and then mantle metasomatism [6]. Mantle metasomatism is characterized by the new minerals formed after the primary paragenesis of peridotites. We should also note the formation of a new generation of spinel [2], as well as overgrowth of clinopyroxene with a variety with higher calcium content [1].

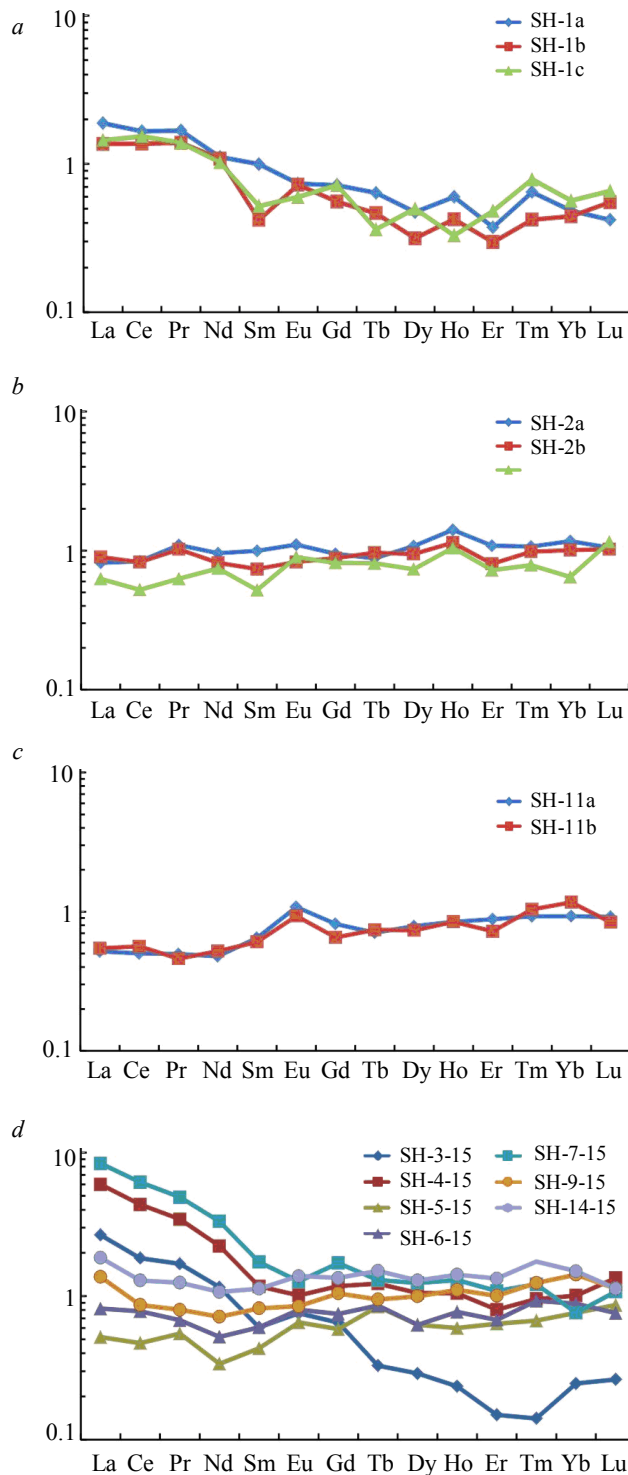


Fig. 1. The chondrite (CI)-normalized REE spectra in the mantle xenoliths of the Svalbard archipelago: *a, b, c* – big xenoliths; *d* – small xenoliths

Analytical techniques. Preliminary all xenoliths have been thoroughly cleared from host basalts by cutting the crusts from the external borders. Since all xenolith samples were ellipsoidal, they were cut along the long axis with subsequent sampling from one part of the xenolith to produce transparent polished sections for petrographic and microprobe analysis. Additional samples were also collected from the same part of the xenolith to study its composition.

The analysis of xenoliths for trace and rare earth elements (REE) was carried out by inductively coupled plasma mass spectrometry (ICP-MS) on an ELAN-DRC-6100 quadrupole mass spectrometer according to the standard method (VSEGEI). The relative measurement error did not exceed 5-10 %.

The content of the major chemical elements in the minerals was determined on a JEOL JSM-6510LA scanning electron microscope with a JED-2200 EDS detector in the laboratory of IPGG RAS. Thin polished rock plates were carbon-covered. A local analysis of the minerals composition was carried out using an electron beam with an accelerating voltage of 20 kV and a current of 1 nA, the beam spot was 3 μm . The accumulation time of each spectrum was 35 s; natural minerals, pure oxides, and metals were used as standards. To correct the matrix effect, the ZAF algorithm was used.

The content of trace and rare-earth elements in minerals and glasses was determined by secondary ion mass spectrometry (SIMS) on a Cameca IMS-4f ion microprobe (Valiev Institute of Physics and Technology of RAS, Yaroslavl branch) in accordance with the methodology described by Sobolev and Batanova [4]. Analyzes were carried out in flat-polished thin sections with gold coating. Cameca IMS-4f (YP FTIAN) experimental conditions: primary ion

beam 16O^{2-} , beam diameter $\sim 20\ \mu\text{m}$; ion current 5-7 nA; primary beam accelerating voltage is 15 keV; relative measurement error does not exceed 10-15 % for most elements. The trace element composition of rock-forming minerals was determined as close as possible to the analytical points of the major elements measured on an electron microprobe. The spectra of REE content in the rocks was normalized to the composition of CI chondrite [11]. List of mineral abbreviations is given by Whitney and Evans [14].

Results and discussion. The distribution spectra of REE in the studied peridotite xenoliths from the Sverre volcano are quite different, however, in all samples, LREE prevails over HREE. Since the xenoliths samples SH-1, SH-2, and SH-11 were quite big, this allowed us to study the distribution of trace elements in different xenolith parts: center, intermediate, and marginal zones. For big xenoliths, REE spectra were plotted separately (Fig. 1).

Within the studied samples, the maximum and minimum contents of LREE differ in different samples by almost an order of magnitude (Table 1). The minimum LREE content of 1.2 ppm is observed in SH-11a sample, and the maximum of 12.5 ppm is found in sample SH-7. It should be noted that both low and high values of the LREE content are in general anomalous for lherzolites [3].

Table 1

Content of REE and trace elements (ppm) in mantle xenoliths of the Svalbard archipelago

Component	SH-1			SH-2			SH-11		SH-3-15	SH-4-15	SH-5-15	SH-6-15	SH-7-15	SH-9-15	SH-14-15
	a	b	c	a	b	c	a	c							
La	0.69	0.50	0.53	0.30	0.33	0.23	0.19	0.20	0.98	2.20	0.19	0.30	3.08	0.50	0.68
Ce	1.59	1.31	1.47	0.80	0.79	0.50	0.48	0.54	1.76	4.16	0.45	0.75	5.95	0.83	1.23
Pr	0.23	0.19	0.19	0.15	0.14	0.09	0.07	0.06	0.23	0.47	0.08	0.09	0.67	0.11	0.17
Nd	0.79	0.77	0.73	0.68	0.58	0.53	0.34	0.37	0.82	1.59	0.24	0.37	2.36	0.51	0.76
Sm	0.23	0.10	0.12	0.23	0.17	0.12	0.15	0.14	0.14	0.27	0.10	0.14	0.40	0.19	0.26
Eu	0.06	0.06	0.05	0.10	0.07	0.08	0.09	0.08	0.07	0.09	0.06	0.07	0.11	0.07	0.12
Gd	0.22	0.17	0.22	0.29	0.27	0.25	0.25	0.20	0.20	0.36	0.18	0.23	0.52	0.32	0.41
Tb	0.04	0.03	0.02	0.05	0.06	0.05	0.04	0.04	0.02	0.07	0.05	0.05	0.08	0.06	0.09
Dy	0.18	0.12	0.19	0.41	0.36	0.28	0.30	0.28	0.11	0.40	0.24	0.24	0.47	0.38	0.49
Ho	0.05	0.04	0.03	0.12	0.10	0.09	0.07	0.07	0.02	0.09	0.05	0.07	0.11	0.09	0.12
Er	0.09	0.07	0.12	0.27	0.20	0.18	0.22	0.18	0.04	0.20	0.16	0.17	0.27	0.25	0.33
Tm	0.02	0.02	0.03	0.04	0.04	0.03	0.03	0.04	<0.01	0.03	0.02	0.03	0.04	0.04	0.06
Yb	0.12	0.11	0.14	0.29	0.25	0.16	0.23	0.29	0.06	0.25	0.19	0.22	0.19	0.35	0.37
Lu	0.02	0.02	0.03	0.04	0.04	0.04	0.04	0.03	0.01	0.05	0.03	0.03	0.04	0.04	0.04
U	0.03	0.02	0.03	0.02	0.02	0.49	0.04	0.07	0.01	0.03	0.09	0.03	0.02	0.03	0.03
Cr	586	650	622	856	981	651	572	738	714	689	662	782	851	847	898
Rb	0.51	0.29	0.35	0.49	0.48	0.28	0.99	0.46	0.56	0.67	0.98	0.44	0.39	0.46	0.54
Sr	24.4	23.8	24.5	15.4	12.6	11.6	19.1	38.0	8.82	10.2	55.9	12.6	8.58	8.27	16.8
Y	1.10	1.06	1.07	2.59	2.31	1.94	0.54	2.40	1.54	1.80	2.53	2.50	2.11	1.83	3.01
Zr	15.3	14.0	14.0	16.2	15.3	15.7	14.4	15.6	14.7	15.2	14.7	15.2	16.1	14.4	16.7
Nb	0.26	0.21	0.24	0.30	0.17	0.11	0.97	0.20	0.16	0.25	0.87	0.09	0.15	0.11	0.14
Ba	16.7	16.2	16.9	18.2	16.0	14.2	22.7	32.6	14.4	16.0	51.0	15.6	14.3	16.4	17.5
La/Yb	5.75	4.55	3.79	1.03	1.32	1.44	0.83	0.69	16.1	8.80	1.00	1.36	16.21	1.43	1.84
LREE	3.53	2.87	3.04	2.16	2.01	1.47	1.23	1.31	3.93	8.69	1.06	1.65	12.46	2.14	3.10
HREE	0.80	0.64	0.82	1.61	1.38	1.16	1.28	1.22	0.52	1.54	0.98	1.11	1.83	1.61	2.03
Eu/Eu*	0.86	1.48	0.97	1.14	1.02	1.34	1.47	1.48	1.20	0.86	1.28	1.19	0.74	0.91	1.12
Ce/Ce*	0.93	1.00	1.09	0.87	0.86	0.83	0.99	1.12	0.85	0.92	0.88	1.05	0.94	0.80	0.83

Note: a – central; b – intermediate; c – marginal part of the samples.

A fairly pronounced differentiation of REE is observed in sample SH-1 (Fig. 1, a). The total content of REE is relatively low. Maximum values are observed in the central part. Upon transition from the xenolith centre to its edge, the REE concentration, in particular, LREE, decreases significantly. The ΣLREE decreases from the center to the edge, having a maximum value of 3.6 ppm in the SH-1a sample and a minimum value of 3.1 ppm in the SH-1c sample. The distribution of HREE in this sample is quite complex, mainly its content decreases from the central part of xenolith to the

intermediate, and then increases. The final increase can be significant in some cases (Table 1). However, the La/Lu ratio decreases from the center to the edge. All parts of big xenolith are characterized by insignificant values of negative Ce and Eu anomalies. The absence of a strong negative Ce anomaly indicates the absence or minimal effect of surface and meteoric waters on xenoliths, which makes it possible to exclude the influence of exogenous processes on the mantle matter carried up to the surface.

REE in the SH-2 sample are also rather weakly differentiated (Fig.1, b). Samples SH-1 and SH-2 are generally similar in REE distribution. Sample SH-2 also shows a decrease in the REE content from the center to the edge, with following average contents values: 0.3, 0.24, and 0.18 ppm in the central, intermediate, and marginal parts, consequently. The only exception, as well as in the case of SH-1 sample, is Lu showing the inverse relation (Table 1). The REE content in sample SH-2 is characterized by subchondritic values. Sample SH-2 is characterized by a weak positive Eu-anomaly and a slight negative Ce-anomaly (Table 1). Thus, the influence of exogenous processes is not observed in this xenolith either.

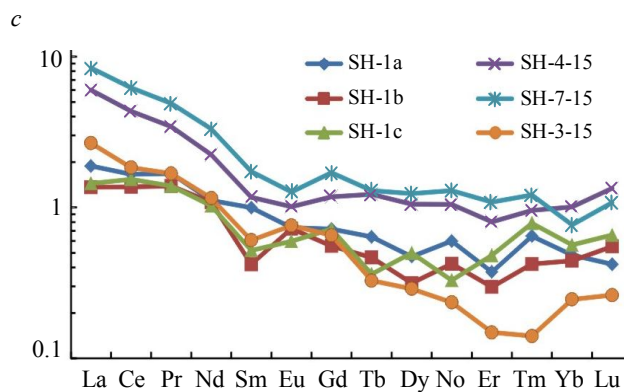
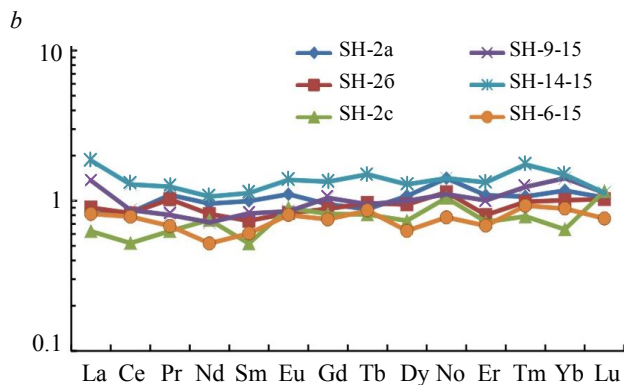
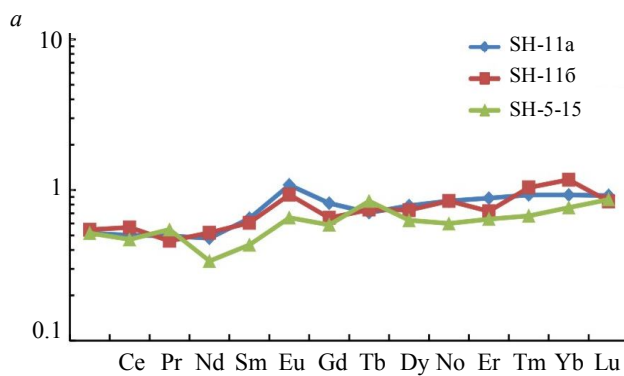


Fig.2. Classification of REE chondrite-normalized spectra in mantle xenoliths of the Svalbard archipelago: a – first; b – second; c – third types

REE in the composition of sample SH-11 are slightly differentiated (Fig.1, c). Sample SH-11 is smaller than the two abovementioned, so we analyzed only the central and marginal parts (Table 1). The distribution of LREE and HREE practically does not differ in the central and marginal parts. The sample is characterized by a positive Eu-anomaly ($Eu/Eu^* = 1.48$). As in the larger xenoliths, there is no Ce-anomaly (Table 1).

Other xenolith samples (SH-3, SH-7, SH-9, SH-14) are small. This group of xenoliths is rather heterogeneous in the REE content; samples SH-4 and SH-7 stand out from the current set (Fig.1, d). Samples SH-4 and SH-7 contain LREE 5 times more than other xenoliths. The HREE content in SH-4 and SH-7 is almost the same as in the other five xenoliths, and in some cases lower. Samples SH-4 and SH-7 are characterized by weak negative Ce- and Eu- anomalies; in the remaining samples, the anomalies are also weak and positive (Table 1).

The considered mantle peridotites can be attributed to the three types proposed by F.P.Lesnov [3] based on the summarizing of a significant amount of analytical data on the geochemistry of mantle rocks. This classification is based, first of all, on the La/Lu ratio, which reflects the degree of REE fractionation. The first type is characterized by La/Yb rate value <1 , and a positive slope of the REE spectrum. The second type is marked by a La/Lu ratio values close to 1 and the subhorizontal REE spectra. The third type has La/Lu ratios value >1 and a negative slope of the REE spectra (a noticeable enrich-

ment in LREE in relation to HREE). The use of this classification can help answer the question: did basaltic melt affect xenoliths during their transportation? If such an impact took place, then a similarity of REE spectra should be observed in all samples of mantle peridotites.

Big xenolith SH-11 can be attributed to the first type. In both parts of this xenolith, weak LREE depletion is observed, due to which REE spectra have a barely noticeable positive slope and are characterized by La/Yb ratios of less than 1. This sample extremely stands out from others in the specific features of the trace elements content (Fig.2, *a*, Table 1) and has similarities with peridotites from massifs distributed within the folded areas on platforms, from the MORB zone, as well as from ophiolites [3].

The second type in contrast to the first one, includes xenoliths slightly enriched in LREE. Such xenoliths from the studied collection are SH-2, SH-5, SH-6, SH-9, and SH-14. Compared with the first type, these samples have an almost subhorizontal REE spectrum, and the La/Yb ratio tends to unity (Fig.2, *b*).

Xenoliths, which are the most specific in their geochemical characteristics, belong to the third type (Fig.2, *c*). All of them are abnormally enriched in LREE, therefore REE spectra have a very steep negative slope and are characterized by a high La/Yb ratio, which can reach 52 (Table 1). This type includes SH-1, SH-4, SH-6, and SH-7 samples. Among the xenoliths of this type, the SH-3 sample stands out because of its higher LREE content, exceeding the content in the primitive mantle by a factor of 4, and at the same time, it is depleted in HREE relative to the primitive mantle by about 5 times (Fig.2, *c*).

The mineral composition of the third type xenoliths does not correlate with the REE content in them. The orthopyroxene content in the xenoliths of the third type relative to the first and second ones decreases from 15-19 to 5-7 %. However, the REE content in orthopyroxene from the studied rocks is insignificant (Table 2); therefore, a decrease in the content of this mineral is unable to significantly affect the bulk content of REE.

It should be noted that in all peridotite xenoliths under study, there is no correlation between LREE (in particular, La), and CaO content (Fig.3, *a*). At the same time, a pronounced positive correlation is observed between the CaO content and Yb (Fig.3, *b*), which distinguishes these samples from mantle rocks of other origins [3].

In addition, a correlation was found between the La distribution and the content of a number of HFS and LIL elements. In particular, the highest contents of such impurity elements as U, Sr, Nd, and Ba were noted in xenoliths assigned to the third geochemical type (Fig.4). It was found that the U content in the marginal part of SH-2 xenolith is anomalously high (0.49 ppm, Table 1) and stands out from the set of samples.

The distribution of HREE in the whole set of xenoliths under study is quite sustainable. The major contribution to the Σ HREE is made by Yb (Table 1). In all samples, at the level of increased Yb content, an increase in the content of a number of siderophile ele-

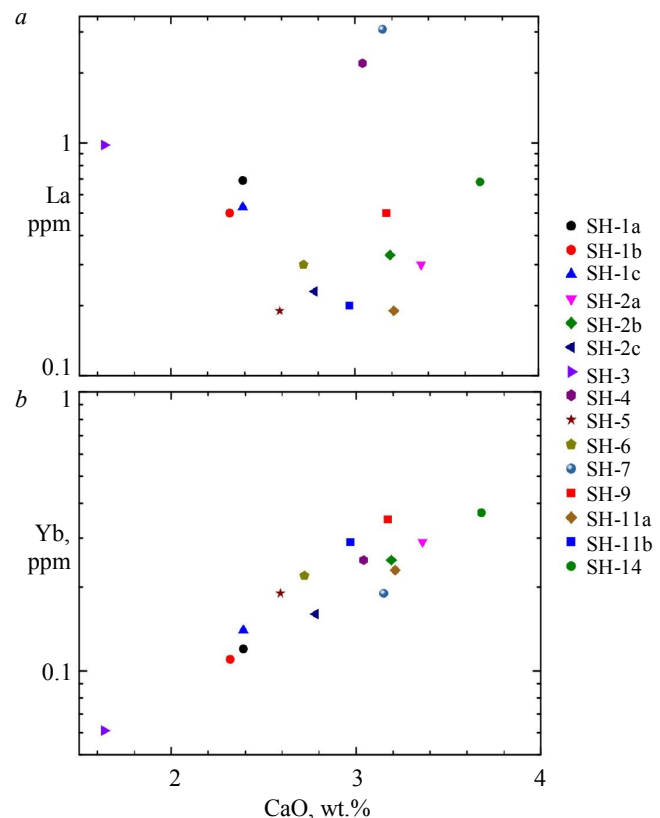


Fig.3. The ratio of CaO and La (*a*), Yb (*b*) contents

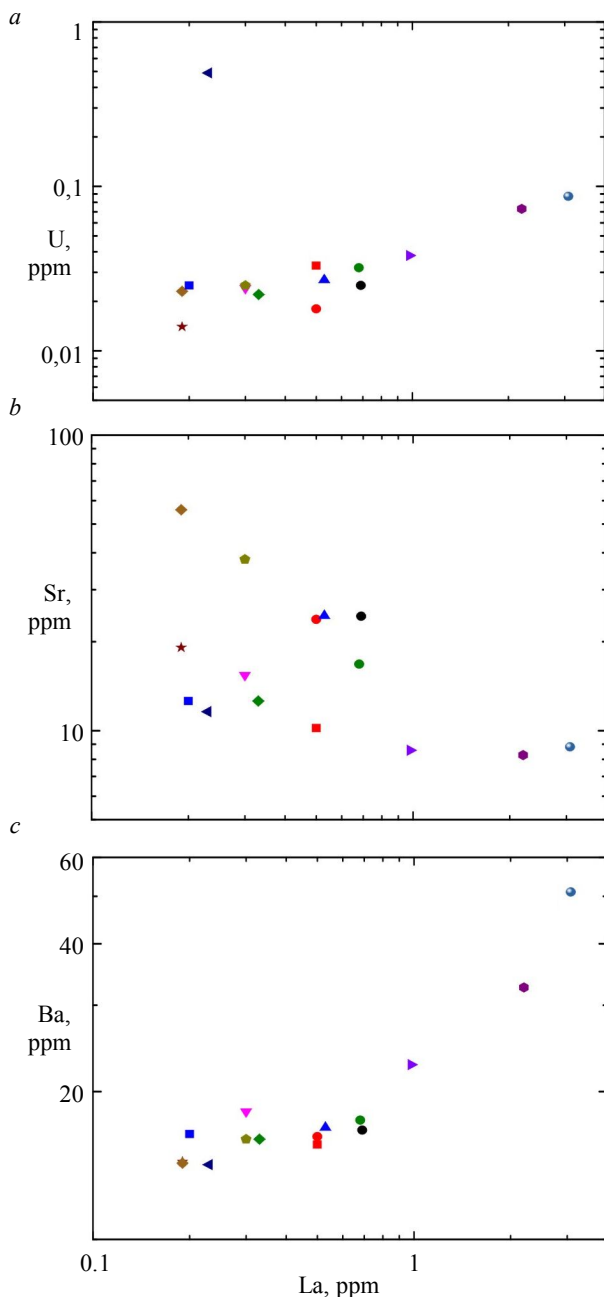


Fig.4. The ratio of the content of La and U (a), Sr (b), Ba (c) (see symbols in Fig.3)

wide range of changes in the content of LREE and other trace elements, fairly constant high concentrations of HREE is observed throughout the samples.

Currently, there are two hypotheses explaining the increased content of trace elements in the mantle rocks.

The first hypothesis suggests connecting the increase in the trace elements content in mantle rocks with the processes of mantle metasomatism. There are two types of mantle metasomatism: evident and stells metasomatism. A characteristic feature of the first type is the dominant effect of the aqueous phase, due to which minerals with the OH-group (phlogopite, amphibole), as well as minerals rich in incompatible trace elements are formed [9, 13]. With stells metasomatism, an increase in the LREE content in mantle rocks is associated with the fluid supply. According to published data, this is a carbonatite fluid enriched in LREE and a number of other incompatible elements [6, 7].

ments Ti, V, and Cr is noticeable. The correlation of these elements is most likely associated with their predominant accumulation in clinopyroxene.

The distribution of trace elements in big xenoliths is similar in general. The same patterns can be traced in samples SH-1 and SH-2, but the content of most of the trace elements in SH-2 is lower (Table 1). The distribution of trace elements in the SH-11 sample is similar to other xenoliths and is characterized by subchondritic values, with the exception of U, Ce, and Yb (Table 1), for which the content was found to be increased by about 1.2 times.

All trace elements in the composition of sample SH-1 have a maximum content in the central and marginal zone. Only Cr shows a decrease in the content from the center to the intermediate part and then increases towards the rim (Table 1).

The distribution of trace elements in small xenoliths is significantly different from big samples. Small xenoliths show an increase in the Th, U, and Ce content by five or more times. In this group, there are samples with high REE content and anomalously high concentrations of the above elements (the exceedance relative to chondrite is up to 10-20 times).

It should be noted that almost all xenolith samples, for which an increased content of trace elements was found, are of the third geochemical type. In particular, this is due to a positive correlation of La and a number of HFS and LIL elements (Fig.4).

The obtained data on the REE and a number of rare elements distribution in the mantle xenoliths of the Svalbard archipelago, along with the literature data [6, 8, 10], allow us to note some geochemical features of this province. Despite a

The second hypothesis suggests enrichment in LREE and LIL elements due to the interaction of xenolith with basalt melt during the mantle rocks transportation to the surface [3]. That hypothesis stated that the main cause for enrichment is the lack of equilibrium in the xenolith–basaltic melt system, while the basaltic melt is much hotter than the mantle that it breaks through. It is evident that the content of incompatible elements, as well as volatile components, is higher in basaltic melts than in the hosting restite. Consequently, basaltic melt, affecting xenolith, increases the content of incompatible elements by filtration metasomatism in its entire volume, and in case of big xenoliths in the marginal part.

When applying this hypothesis to the obtained data, it contradicts the following facts: LREE enrichment is not observed in all xenoliths, and xenolith samples differ quite significantly in the trace elements content. In addition, according to this hypothesis, the greatest enrichment in incompatible elements would be in small xenoliths and in the marginal parts of large ones, which was not confirmed in this study. It can be concluded that most likely enrichment of mantle xenoliths with incompatible elements (LREE, HFSE and LILE) is associated with mantle metasomatism.

It can be assumed that the most probable source of HFS and LIL elements is the melt formed during the partial melting of ortho- and clinopyroxene in mantle rocks, previously prepared under the influence of a mantle fluid that lowers the melting temperature. These processes are consistent with a decrease in the orthopyroxene content level in xenoliths of the third type, as well as with a change in the clinopyroxene composition in the marginal zone (Fig.5). Apart from the orthopyroxene content reduction, it is also worth noting changes in its morphology according to electron microscopy study. Often the grains of this mineral have traces of melting, as well as corroded border areas. It is also noted the replacement of orthopyroxene by clinopyroxene (Fig.5). Apparently, it is the melting of orthopyroxene under the influence of the mantle fluid, as well as the partial melting of the clinopyroxene that leads to the formation of a melt of the basic composition. Such a hypothesis was considered by G.B.Fershtater [5] by the case of mantle xenoliths in alkaline basaltoids from Makhtesh Ramon, Israel.

Table 2 shows the averaged compositions of ortho- and clinopyroxene, glass, and also host basalts. The glass contains much more silica than basalt, so it cannot be considered as a result of an injection of basalt melt into

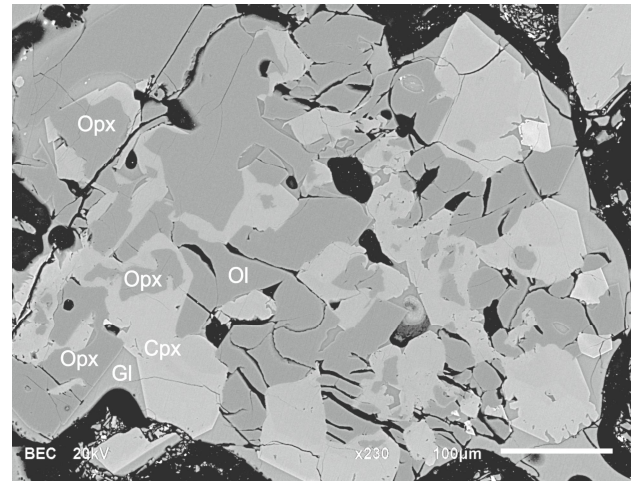


Fig.5. BSE image of the melt pocket in peridotite xenolith recording the result of the orthopyroxene (Opx) partial melting with the formation of glass (Gl) accompanied by a change in the olivine (Ol) and clinopyroxene (Cpx) composition

Table 2

Content of major and rare earth elements in pyroxenes, glass and basalt

Component	Opx n = 11	Gl n = 8	Cpx n = 10	Basalt n = 2
SiO ₂	56.87	52.41	51.13	41.25
TiO ₂	–	1.93	0.78	2.47
Al ₂ O ₃	3.34	24.23	6.38	12.20
Cr ₂ O ₃	0.42	0.05	1.34	0.04
FeO	5.99	3.55	2.72	11.35
MnO	0.15	0.05	0.13	0.16
MgO	32.69	2.02	14.52	11.45
CaO	0.54	7.39	22.01	9.48
La	0.01	29.9	8.68	51.5
Ce	0.04	63.4	23.5	90.1
Pr	0.01	7.39	3.38	9.98
Nd	0.05	30.9	17.8	36.7
Sm	0.04	5.32	4.27	7.41
Eu	0.01	1.70	1.49	2.50
Gd	0.04	5.30	4.51	7.31
Dy	0.08	4.91	4.37	5.13
Er	0.12	3.26	2.78	2.35
Yb	0.20	3.18	2.62	1.69
Lu	0.03	0.48	0.36	0.26

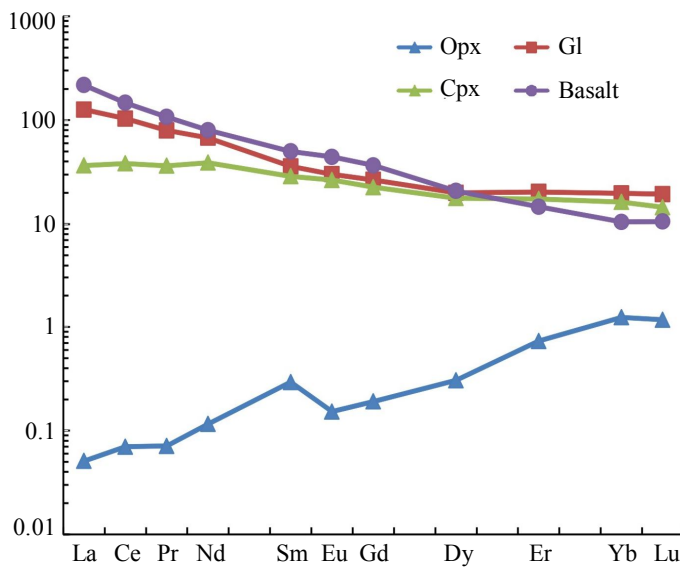


Fig.6. Chondrite-normalized REE spectra in orthopyroxene, glass, clinopyroxene, and basalt

xenolith. The distribution of REE in all four phases is quite informative. It is worth noting the similarity of the REE spectra in clinopyroxene, glass, and basalt (Fig.6). The observed depletion of orthopyroxene in LREE is not typical for this mineral [3]. According to published data, the U-shaped REE spectra is most characteristic of orthopyroxene. In orthopyroxene from xenoliths of the Sverre volcano, the spectrum has a pronounced positive slope from LREE to HREE, indicating a depletion in LREE. Such behavior of LREE in rock-forming minerals participating in migration processes during partial melting in the presence of fluid was noted earlier [2, 12].

Conclusions. Thus, the proposed mechanism for the enrichment of mantle

peridotites xenoliths with incompatible elements (LREE, HFSE, and LILE) is associated with the mantle metasomatism. The most likely source of HFS and LIL elements in mantle rocks is the infiltrate obtained as a result of the interaction of the fluid with upper mantle rocks. The presented data indicate that mantle rocks of the Svalbard archipelago may have made a significant contribution to the formation of basaltic melt due to the melting of ortho- and clinopyroxene. When xenoliths of mantle peridotites were carried to the surface, the effect of transporting basaltic melt was minimal.

REFERENCES

1. Ashikhmin D.S., Skublov S.G., Mel'nik A.E., Sirotkin A.N., Alekseev V.I. Geochemistry of rock-forming minerals in mantle xenoliths from basalts of Sverre Volcano, Spitsbergen Archipelago. *Geochemistry International*. 2018. N 8, p. 857-864.
2. Ashikhmin D.S., Chen Yu.-S., Skublov S.G., Mel'nik A.E. Geochemistry of spinels from xenoliths of mantle lherzolites (Sverre Volcano, Spitsbergen Archipelago). *Zapiski Gornogo instituta*. 2017. Vol. 227, p. 511-517. DOI: 10.25515/PMI.2017.5.511 (in Russian).
3. Lesnov F.P. Rare earth elements in ultramafic and mafic rocks and their minerals. Main types of rocks. Rock-forming minerals. CRC Press/Balkema, 2010, p. 587.
4. Sobolev A.V., Batanova V.G. Mantle lherzolites of the Troodos ophiolite complex, Cyprus-clinopyroxene geochemistry. *Petrologiya*. 1995. Vol. 3. N 5, p. 440-448.
5. Fershtater G.B., Yudalevich Z.A., Khiller V.V. Xenoliths in the alkali basalts of Makhtesh Ramon of Desert Negev (Israel) as indicators of mantle metasomatism and magma generation. *Lithosphere (Russia)*. 2016. N 3, p. 82-111 (in Russian).
6. Ionov D.A., O'Reilli S.Y., Genshaft Y.S., Kopylova M.G. Carbonate-bearing mantle peridotite xenoliths from Spitsbergen: phase relationships, mineral compositions and trace element residence. *Contributions to Mineralogy and Petrology*. 1997. Vol. 125, p. 375-392.
7. Dupuy C., Liotard J.M., Dostal J. Zr/Hf fractionation in intraplate basaltic rocks: carbonate metasomatism in the mantle source. *Geochimica et Cosmochimica Acta*. 1992. Vol. 56, p. 2417-2423.
8. Frey F.A., Haskin L.A., Haskin M.A. Rare earth abundances in some ultramafic rocks. *Journal of Geophysical Research*. 1971. Vol. 76, p. 2057-2070.
9. Frey F.A., Prinz M. Ultramafic inclusions from San Carlos, Arizona: petrologic and geochemical data bearing on their petrogenesis. *Earth and Planetary Science Letters*. 1978. Vol. 38, p. 129-176.
10. Ionov D.A., Ashchepkov I.V., Stosch H.G. et al. Garnet peridotite xenoliths from the Vitim volcanic field, Baikal region: The nature of The garnet – Spinel peridotite transition zone in the continental mantle. *Journal of Petrology*. 1993. Vol. 34, p. 1141-1175.
11. McDonough W.F., Sun S.S. The composition of the Earth. *Chemical Geology*. 1995. Vol. 120, p. 223-253.
12. Stachel T., Viljoen K.S., Brey G., Harris J.W. Metasomatic processes in lherzolitic and harzburgitic domains of diamondiferous lithospheric mantle: REE in garnets from xenoliths and inclusions in diamonds. *Earth and Planetary Science Letters*. 1998. Vol. 159, p. 1-12.



13. Roden M.F., Frey F.A., Francis D.M. An example of consequent mantle metasomatism in peridotite inclusions from Nunivak Island, Alaska. *Journal of Petrology*. 1984. Vol. 25, p. 546-577.
14. Whitney D.L., Evans B.W. Abbreviations for names of rock-forming minerals. *American Mineralogist*. 2010. Vol. 95, p. 185-187.

Authors: **Dmitriy S. Ashikhmin**, 1 category geologist, Dmitry_Ashikhmin@vsegei.ru (A.P.Karpinsky Russian Geological Research Institute, Saint-Petersburg, Russia), **Sergey G. Skublov**, Doctor of Geological and Mineralogical Sciences, Chief Researcher, skublov@yandex.ru (Institute of Precambrian Geology and Geochronology RAS, Saint-Petersburg, Russia).

The paper was received on April 17, 2019.

The paper was accepted for publication on May 30, 2019.